

Supplementary Information

Neuronal correlates of decision-making in secondary somatosensory cortex.

By

Ranulfo Romo, Adrian Hernandez, Antonio Zainos, Luis Lemus, Carlos Brody

Contents

1. First stimulus and inter-stimulus activity	1
2. S2 activity leads M1 activity in the vibrotactile discrimination task	3
3. Quality of planar fits	5
4. Muscle activity during and after the second stimulus (f2)	6
5. Stimulus-dependent firing rates, or stimulus-dependent latencies?	8

1. First stimulus and inter-stimulus activity.

We document here the first stimulus and interstimulus delay period responses of S2 neurons during the vibrotactile discrimination task. A previous paper (ref. 8, Salinas *et al.*, *J. Neurosci.* 2000) has reported similar analyses for a set of recordings overlapping with the ones reported here. The main results regarding the interstimulus delay period are: (1) Some neurons in S2 carry an f1-dependent signal during the first 500 ms or so of the delay period, but this signal weakens very rapidly thereafter, and by the time some 1500 ms of the delay period have elapsed, all traces of f1-dependence have completely disappeared from the firing rates. (2) A very small number of neurons in S2 show an f1-dependence again some tens of milliseconds before the end of the interstimulus delay period, in anticipation of the second stimulus.

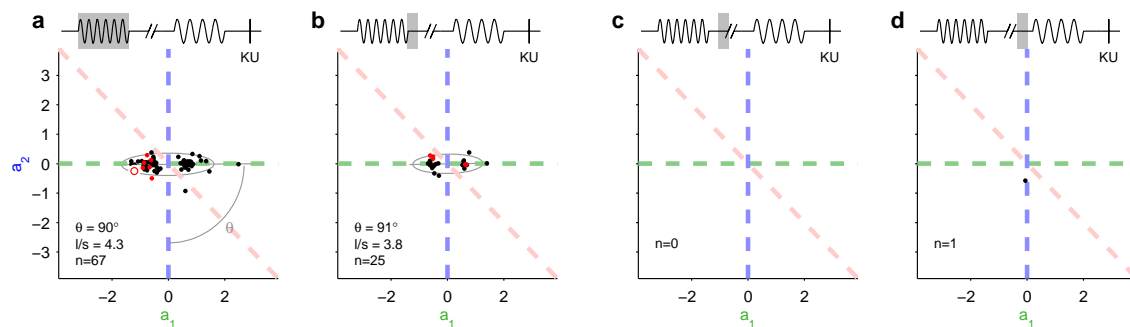


Figure S1: Analysis of first stimulus and delay period activity using the same procedures and format as in Figure 6 of the main manuscript. Grey boxes above each panel schematically indicate the time window analyzed (delay period in schematic not to scale). Grey ellipses are a Gaussian fit to the distribution of data points shown. Only data points significantly different to (0,0) are shown in each panel (significance level is $P < 0.01$; see Methods). Red data points correspond to same neurons identified with red dots in Fig 4 of the main manuscript. **a:** first stimulus period. **b:** first 500 ms of inter-stimulus delay period. **c:** from 500 ms to 1000 ms of delay period. **d:** from 2000 to 2500 ms of delay period.

We analyzed delay period data with both the planar fit method described in the current paper (see Figure S1), and a very similar method, designed to focus specifically on f1-dependence in delay period responses. The latter method was used in a previous paper that reported stimulus-dependent delay period responses in prefrontal cortex (PFC) during the same task (Romo *et al.*, *Nature* 1999; see Figure S2 below). Both of these similar methods gave the same results.

The planar fit method used in the main manuscript (firing rate = $a_1 \cdot f_1 + a_2 \cdot f_2 + \text{const.}$) is applied to delay period responses in Figure S1 above. As can be seen in panel a, responses to the first stimulus (f1) cluster closely along the $a_2=0$ line, indicating that the responses depend only on the first stimulus—exactly as we expect. During the first 500 ms of the delay period (panel b), significant numbers of neurons are found to still respond with firing rates that are a function of f1. But after this, the number of neurons detected as having coefficients significantly different to (0,0) falls to chance. The same 517 neurons analyzed in the main text were analyzed in Figure S1.

We also applied a method previously used in a paper focusing on f1-dependent delay period responses (ref. 12, Romo *et al.*, *Nature* 1999; see Methods therein). Figure S2 below was created using the same methods as Figure 3g in that paper. The y-axis shows the number of neurons with a significantly f1-dependent firing rate, as a function of time, in steps of 20 ms. (Before analysis, firing rates were smoothed with Gaussian kernels of width $\sigma=50$ ms in the stimulus period, $\sigma=150$ ms in the delay period. During the delay period, the analysis is thus roughly equivalent to displaying the results of a 450 ms-wide window, slid forward in time in steps of 20 ms.)

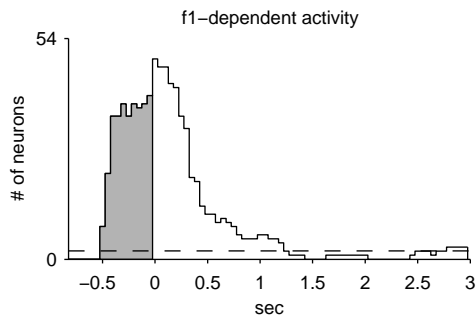


Figure S2: Number of f1-dependent neurons as a function of time. The methods of Figure 3g in ref. 12 (Romo *et al.*, *Nature* 1999) were applied to data from cortical area S2. First stimulus period runs from -0.5 s to 0 s (shaded grey in histogram), and interstimulus delay period length is 3 s. Second stimulus responses not shown. Y-axis shows number of neurons found to have firing rates significantly dependent on f1 as a function of time; individual neurons may participate in more than one time bin. Dashed horizontal line indicates chance level (significance level here is $P < 0.04$, see Methods of ref. 11). After about 1500 ms of the delay period, the number of f1-dependent neurons has fallen to chance.

Towards the end of the delay period, a few neurons appear to become f1-dependent again. Although their number is close to that expected by chance at a $P < 0.04$ significance level, some of them are significant at a much more stringent level. Figure S3 shows the single clearest example of such a neuron, which is similar to neurons we described in PFC and dubbed ‘late’ neurons. This neuron achieved significance at a $P < 0.0001$ level.

Neurons such as that shown in Figure S3 were rare, but, as in the example shown, clearly present. Since many of our experiments were conducted in blocks of trials with a fixed interstimulus interval, the monkey was able to get used to the rhythm of the task and anticipate the timing of the second stimulus. The neuron shown in Figure S3 is extreme in that (a) its anticipatory f1-dependence starts some 500 ms before the second stimulus; most such neurons found in cortical area S2 began their f1-dependence much later, typically some 100 ms or only tens of ms before

the second stimulus; and (b) most such neurons had a much weaker f1-dependence, before the second stimulus started, than the clear example shown here.

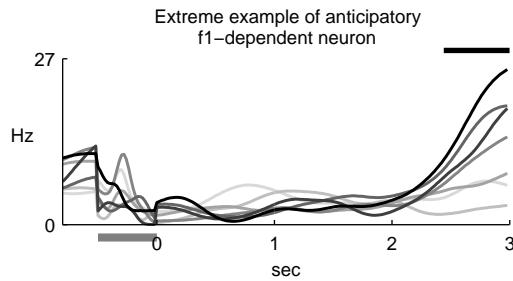


Figure S3: Smoothed peristimulus time histograms (PSTHs) of spike trains of a single neuron during the first stimulus and interstimulus delay period of the vibrotactile discrimination task. First stimulus is indicated by thick horizontal grey bar, and runs from -0.5 s to 0 s; delay period is 3 seconds long. Grey level codes for f_1 , vibrotactile frequency of applied first stimulus, and runs, in steps of 4 Hz, from 10 Hz (lightest grey line) to 34 Hz (darkest black line). Thick horizontal dark line above plot indicates time bins where significant f_1 -dependence was found, at a $P < 0.04$ significance level.

2. S2 activity leads M1 activity in the vibrotactile discrimination task.

The main result described in this section is that decision-related activity in cortical area S2 occurs before decision-related activity in primary motor cortical area M1. This argues that the decision-related activity in S2 is not being driven by a motor efference copy signal from M1.

As described in the main text, the activity in some somatosensory cortical area S2 neurons is closely correlated with the animal's decision-reporting motor act; we conclude that this activity is therefore correlated with the animal's decision. This correlative observation, while correct, nevertheless allows the interpretation that decision-correlated activity in S2 does not causally lead to the animal's decision, but may instead be driven by an efference copy of the motor instruction. In other words, in this interpretation, activity in motor areas causes decision-correlated activity in S2, not the other way around. Two control experiments were performed to check this possibility.

First, as documented in the main text (Figures 4e and 4f), seventeen S2 neurons were recorded during a visual instruction task in which the animal performed the same motions as in the standard vibrotactile discrimination task, but was guided by visual cues, not somatosensory ones (see Methods). Under these conditions, no statistically detectable correlation with the animal's motor act was found. We conclude from this that there is no straightforward link between activity in motor areas and decision-related activity in S2. At the very least, any such link must be firmly gated by the somatosensory task, since without this task, the correlation with the motor act is unobservable. Such gating would be natural and to be expected if S2 participates in decision-making during the vibrotactile discrimination task, but not during the visual task—our preferred interpretation. Such gating would otherwise be much harder to explain, although it could still not be ruled out.

Second, however, we recorded, in separate experiments, from one of the same monkeys, during the same task, from primary motor cortical area M1. Our goal was to compare the latency of responses in M1 with the latency of responses in S2. If activity in M1 were driving S2, we would expect the latency in M1 to be shorter than S2; if a third (premotor) area were driving both M1 and S2, we would expect latencies in M1 and S2 to be similar. But if activity in S2 were directly or indirectly driving M1, we would expect latencies in S2 to be shorter than in M1.

Since the recordings in M1 were carried out at a different time as the ones in S2, we first checked for any evidence that the monkey was performing the task differently during the two sets of recordings (S2 vs. M1). We found no significant difference in error rates, and when we compared the distributions of reaction times (time between the end of the second stimulus and the KU event; see Fig. 1a), we found that neither the means, medians, nor even whole distributions were significantly different (t-test, Wilcoxon test, Kolmogorov-Smirnov test respectively, $p > 0.5$ for all three; mean \pm standard error of reaction times during recordings in S2 for this monkey was 326 ± 7 ms, during recordings in M1 it was 330 ± 9 ms). We therefore concluded that the monkey, which had been highly trained before any recordings started, was performing the task in a highly consistent and stereotyped manner across the two sets of recordings.

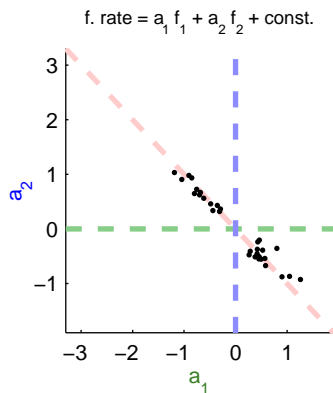


Figure S4. Planar fits for data from primary motor cortical area M1. Format is identical to Figure 4a of main manuscript. As in Figure 4a, firing rates analyzed for each neuron (one neuron per data point) were obtained from averaging over the entire 500 ms-long second stimulus period.

We then analyzed neuronal responses in M1 during the second stimulus period, using the planar fit method as in Figure 4a of the main text (see Figure S4 below). As can be seen in the Figure, the data points for M1 neurons cluster extremely closely to the $a_2 = -a_1$ diagonal line. This is what one would expect from neurons with a response that depends only on the monkey’s final decision as to which of the two pushbuttons to press (that is, during correct trials, the response depends only on the sign of $f_1 - f_2$). All neurons of M1 began, and maintained throughout their significant stimulus-dependent response, a response that was best described as a function of $f_1 - f_2$. Thus, in terms of their response dependence, all these neurons were similar to the neurons that we described in the main text as “diagonal” neurons.

We then analyzed the latency of these diagonal responses (relative to the beginning of the second stimulus), using exactly the same criteria as was used for the neurons in S2 (see Methods). For the most direct comparison between equivalent types of responses, we chose to compare the M1 neurons against the S2 neurons we had found that also began their stimulus-dependent response as functions of $f_2 - f_1$, i.e., neurons that were initially “diagonal”. We found that the latencies of these neurons in S2, in the same monkey, during the same task, were significantly shorter than those in M1, by almost 60 ms ($P < 0.03$, one-sided t-test):

Mean latency of diagonal neurons in S2: 236 ± 21 ms (mean \pm standard error)

Mean latency of diagonal neurons in M1: 295 ± 20 ms

Moreover, we found that 30% of the diagonal neurons in S2 in this monkey had latencies that were shorter than the very shortest latency of all the M1 neurons; a permutation test, to see

whether this could occur under the null hypothesis that both sets of latency measurements were drawn from the same distribution, found that this was significant to a $P < 0.004$ level.

We therefore concluded that decision-correlated activity in S2 led decision-correlated activity in M1. This would be best tested in simultaneous recordings from both S2 and M1, and in recordings from more than one monkey, but nevertheless the identical distributions of monkey responses and response times found for both sets of recordings gives us confidence that our results are not due to differences in behavior on the part of the monkey. Our results therefore argue against the hypothesis that the activity in S2 was driven by a motor efference copy signal from M1.

3. Quality of planar fits.

An evaluation of the quality of the planar fits used in the paper showed that these fits were in general a good approximation to the responses of the neurons.

As reported in the main text, firing rates of neurons in S2 were fit as a general linear function of the applied vibrotactile stimulus frequencies (i.e., a plane):

$$\text{Firing rate} \sim a_1 * f_1 + a_2 * f_2 + a_k, \quad (1)$$

where f_1 and f_2 are the frequencies of the first and second stimuli in each trial, respectively, and a_1 , a_2 , and a_k are scalar coefficients to be found by minimizing the sum of the squared difference between the firing rates predicted by the above formula and the firing rates found experimentally.

We chose equation (1) as the simplest possible functional form that could describe firing rate dependence on both f_1 and f_2 . As such, it is intended more as a convenient approximation that allows evaluating functional dependence on f_1 and f_2 rather than an exact description of response properties. For example, equation (1) assumes that there is no response saturation at high-predicted firing rate values.

[Notice, however, that if the responses are actually of a type described by

$$\text{Firing rate} = g(b_1 * f_1 + b_2 * f_2 + b_k), \quad (2)$$

where $g()$ is some nonlinear function describing saturation, then the vector $\mathbf{a} = (a_1, a_2)$ obtained by fitting equation (1) to the responses will be parallel to the vector $\mathbf{b} = (b_1, b_2)$. This is because, in (f_1, f_2) space, lines of equal firing rates will be formed perpendicular to \mathbf{b} ; therefore \mathbf{a} will either be identically zero or perpendicular to these lines, in which case it must necessarily be parallel to \mathbf{b} . Thus the relative functional dependence, that is, strength of dependence of responses on f_1 vs. strength of dependence on f_2 , will still be accurately reported by the fit obtained through equation (1).]

We have previously reported that firing rates of S2 neurons during the first stimulus period of this task are well described by *monotonic* functions of f_1 (ref. 8, Salinas *et al.*, *J. Neurosci.* 2000). Non-monotonic tuning was not found to any significant extent. Assuming this generalized to the second stimulus, we therefore expected that the relative dependence on f_1 and f_2 obtained through fitting equation (1) would be a good approximation to the true functional dependence. One very simple way to check this is by asking how well the planar fits account for the data. Following ref. 32, for each fit we computed Q , the “quality of the fit,” that is, the probability that

the data points found experimentally would be obtained if produced by the fit model (equation 1) with Gaussian noise of a standard deviation matching that found experimentally. Panel a of Figure S5 shows the result. The vast majority of the fits had high Q values: 70% of the fits had $Q > 0.1$, and 80% of them had $Q > 0.05$. From this we concluded that our goal of describing functional dependence on f_1 and f_2 was very satisfactorily achieved with the simple planar fit method.

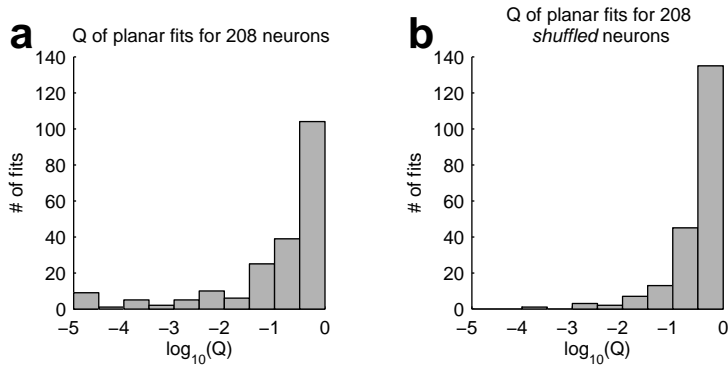


Figure S5. Probability Q that data found experimentally would be found under the planar fit model of equation 1 (one fit for each neuron; for methods to obtain Q , see ref. 32). Data shown is for the fits of Figure 4a of the main text. **a.** Experimental data. Eighty percent of the fits have a $Q > 0.05$. **b.** Results of identical procedure for data after shuffling f_1 , and f_2 stimulus labels within each neuron’s data record. Ninety percent of these fits have a $Q > 0.05$.

However, to compare the distribution of Q s shown in Figure S5a with what would be expected if the planar fit model were in fact exactly correct, we also obtained the distribution of Q s after fitting data in which the stimulus frequency labels, f_1 and f_2 , had been randomly shuffled among the different trials of each neuron’s record. For this shuffled data set, there is no consistent relationship between firing rate and f_1 and f_2 , which means that the exactly right model is in fact the planar fit with $(a_1, a_2) = (0, 0)$. The distribution of Q s of such fits is shown in Figure S5b, and can be seen to be fairly similar to that of Figure S5a. The distribution in Figure S5a does have a noticeably stronger tail at small values of Q , with 17 neurons having $Q < 0.001$, compared to only 1 neuron having $Q < 0.001$ in Figure S5b. We therefore examined the data for each of these 17 neurons individually, and found that in 15/17 cases the small Q could be accounted for by simple non-linearities and saturation effects in the firing rates of the neurons (e.g., no negative firing rates). Only in the last 2 cases, 1% of the data set, were non-monotonicities which could invalidate the interpretation of the planar fit found. In sum, the planar fit was a very adequate approximation.

4. Muscle activity during and after the second stimulus (f_2)

To determine whether muscle activity correlated with the monkey’s upcoming decision occurred in the monkey’s free hand, we recorded electromyograms (EMGs) from three sets of arm and forearm muscles while one of our monkeys performed the task. We recorded from the biceps (BIC), triceps (TRI), and the extensor digitorum communis (EDC). We divided trials into two groups, according to which button the monkeys pushed in each trial. The average spike rate for each of these muscle groups is shown in Figure S6.

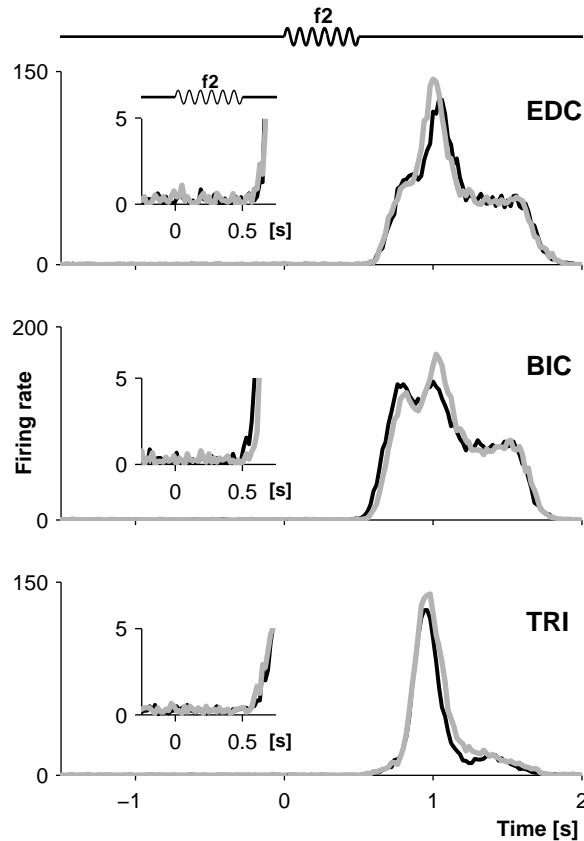


Figure S6. Average spike rates, in spikes/sec, from three different muscle sets in the monkey's free arm used to press the pushbutton indicating the monkey's decision. Grey indicates average over trials where the monkey pushed f2>f1 button; black indicates trials in which the monkey pushed the f2<f1 button. Time=0 indicates start of second stimulus period (f2). Insets show zoom-ins around the time of f2. Top: extensor digitorum communis (EDC). Middle: biceps (BIC). Bottom: triceps (TRI).

Monkeys were trained to wait for the end of f2 before reporting their decision. As can be seen in Fig. S6, there is almost no muscle activity before the end of the f2. Although very low, the activity during f2 itself might still be statistically significantly different for the two pushbutton presses. We therefore carried out t-tests, both for spike rates averaged over the entire f2 period (500 ms), and for spike rates averaged over the last 200 ms of the f2 period, testing for a significant difference between f2>f1 button trials and f2<f1 button trials. In neither of these cases, for none of the three muscle sets, was a significant difference found ($P > 0.1$ for all tests). We therefore concluded that there was no evidence of differential motion in the monkey's free hand that could lead to differential somatosensory signals from that hand.

Our results here coincide with results in a similar, previous, study, where monkeys were asked to categorize the speed of a moving tactile stimulus (Merchant *et al.*, *J. Neurophysiol.* (1997) **77**:1132-1154). Our training procedures for the two tasks were very similar. In the 1997 study, a larger number of muscles groups were recorded from. These included, from the monkey's free arm, the lateral deltoid, anterior deltoid, and from the trunk of the body ipsilateral to the monkey's free arm, the thoracic paraspinal, suprascapular, and infrascapular trapezius muscle groups. As in our present study, none of these showed significant differential activity before the end of the stimulus.

5. Stimulus-dependent firing rates, or stimulus-dependent latencies?

Some neurons, such as the one with responses illustrated in Fig. 2 of the main text and reproduced in Fig. S7 below, showed what appeared to be a systematic relationship between response latency and the applied stimulus frequencies. As described in the main text, the analysis methods used smooth responses in time, either by convolving with a Gaussian (Fig. 5) or with a square window (Figs. 6 and 7). This opens the possibility that systematic differences in response latency within that smoothing window would appear to the analysis as systematic differences in firing rates; thus, while the analysis establishes the relative importance of f_1 and f_2 in determining responses, it does not in itself alone establish which properties of the responses (e.g., firing rate or latency) are the ones that are dependent on f_1 or f_2 .

From visual inspection of the raster plots of many neurons, we expected the main effects to be due to changes in firing rate. To establish this quantitatively, we carried out an analysis, matching that of the main text, in which firing rate was measured completely independently of response latency. For each (f_1, f_2) stimulus pair, we convolved responses with a narrow Gaussian (to avoid edge effects, we used a small σ of 25 ms, but results were identical for $\sigma=45$ ms), and found the moment, within the window running from the beginning of f_2 until 300 ms after f_2 , at which the firing rate reached its maximum. This peak rate was then taken as the response of the neuron to the (f_1, f_2) pair. Notice that peak firing rate, measured this way, does not depend at all on the latency of the responses: spike trains in response to an (f_1, f_2) stimulus pair can be shifted backwards or forwards arbitrarily in time, without changing the peak firing rate they reach. For each neuron, we then fit the peak rate response as a linear function of the stimulus frequencies f_1 and f_2 :

$$\text{Peak firing rate} = a_1 * f_1 + a_2 * f_2 + \text{const.}$$

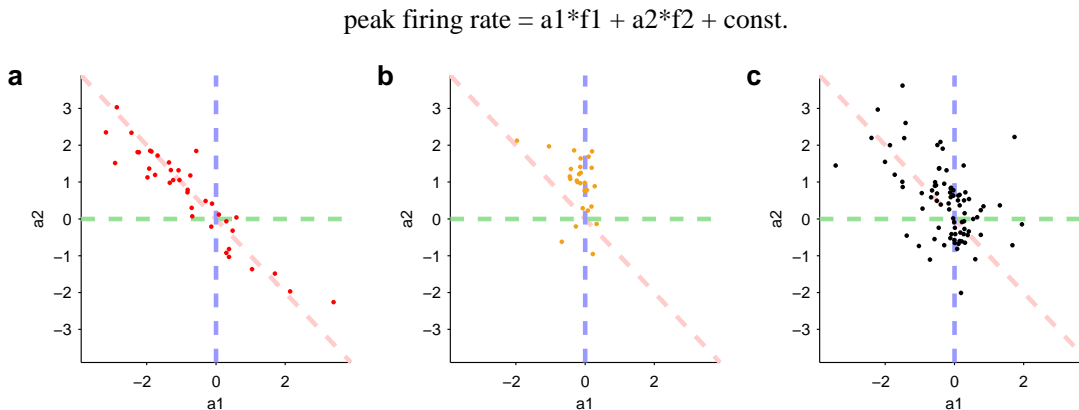


Figure S7. Firing rate modulations, independent of response latency, are a function of the applied stimuli. Here, the peak firing rate, regardless of when after the start of f_2 it occurred, was fit for each neuron as a linear function of stimuli f_1 and f_2 . Each data point represents one neuron. **a**, Neurons classified using the methods of Figs. 6 as $(f_2 - f_1)$ -dependent in the analysis used here. For these neurons, mean time of peak rate after the start of f_2 was 243 ms. **b**, Neurons classified in Fig. 6 as f_2 -dependent remain f_2 -dependent here. Mean time of peak was 221 ms. **c**, neurons classified in Fig. 6 as intermediate. Mean peak rate was 228 ms.

Figure S7 shows the results of this analysis. Neurons have been divided, and color-coded, into the same three groups of Figures 6 and 7. As can be seen, results are very similar, in trends and in

magnitude, as in Figure 6 of the main text. Panel a of Fig. S7 shows fits for neurons that had been classified in Fig. 6 as (f_2-f_1) -dependent. Here, the data points are clustered closely on the $a_2=-a_1$ diagonal, corroborating that these neurons' firing rates, entirely independently of latency, depend on (f_2-f_1) . Similarly, neurons classified in Fig. 6 as f_2 -dependent (shown here in panel b of Fig. S7) are corroborated as having peak firing rates that are largely f_2 -dependent. Finally, neurons of the intermediate group of Fig. 6 are also intermediate in Fig. S7.

The units of the fit coefficients a_1 and a_2 in Fig. S7 are the same as the units in Figs. 4 through 6 (spikes/sec per mechanical pulses/sec, or spikes/pulse). As can be seen by comparing Figs. 6 and S7, the magnitude of the results in Fig. 6 can be very well accounted for the dependence of firing rate on the applied stimulus frequencies, separately from latency.

We therefore concluded that most of our results were due to modulation of firing rates, not latency.

However, this did not rule out that there could be some, perhaps even many, neurons in which latency effects were significant. Unfortunately, although an analysis of firing rate that is completely independent of latency is easily devised (see above), the converse is not so easily done: we were unable to find or devise an analysis that satisfactorily measured latency completely independently of firing rate. After all, response latency is defined as the moment in which a neuron's firing rate abruptly changes, thus inextricably making latency a function of firing rate. For example, consider a latency measure that is the moment at which a firing rate rises above a noise threshold. Two response profiles that have the same temporal shape but are scaled in amplitude with respect to each other would cross that threshold at different times. Thus, even though their temporal shapes are identical, they would be measured as having different latencies. Numerous other obstacles to adequate latency measures exist. For some neurons, some stimulus pairs inhibit firing; for trials in which there are no spikes, no latency is defined (although firing rate is).

For these reasons, we feel our latency analysis to be somewhat unsatisfactory, and have frankly only medium confidence in its results. For completeness, we nevertheless present it here. In contrast to the results of Fig. S7, we found a far less clear relationship between latency and applied stimulus frequencies.

We wished to find a method that detected abrupt increases in firing rates as independently of firing rate magnitude as possible. Reasoning that this was analogous in both spirit as substance to edge-finding methods in computer vision, we applied some basic computer vision methods to finding the response latency for each trial (Horn, 1986, *Robot Vision*). We convolved each spike train with three Gaussians at very different temporal scales, one with $\sigma=12$ ms, one with $\sigma=24$ ms, and one with $\sigma=48$ ms. The result of each of these convolutions was a firing rate estimate at a particular temporal scale. "Edges" in firing rate should correspond to abrupt changes in firing rate, common across all of these temporal scales. We thus searched for zero-crossings of the second derivatives of the results of the three convolutions, and selected those zero-crossings that coincided in time within 25 ms for the two fastest temporal scales, and within 45 ms for the slowest temporal scale. To eliminate noise, we kept only those second-derivative zero-crossings that corresponded to peaks in the first derivative that were more than 1 r.m.s. of the first derivative above zero. Notice that up to now, since we used the r.m.s. of the first derivative itself, there was no parameter setting an explicit firing rate magnitude scale. Thus responses with low firing rates and with high firing rates could both be accommodated by this procedure. However, we found that trials with a single spike led to the time of that spike being defined as the latency. This is

reasonable in the absence of any other spikes, but since most of these single spikes appeared spontaneous and unrelated to the stimulus, we felt they simply reflected noise. Accordingly, we set a minimum peak first derivative at the fastest temporal scale of 400 spikes/sec^2 ; this eliminated single spikes. The first zero-crossing after the start of f_2 to pass all these tests was considered the response onset latency.

Below we present the results of the analysis just described; quantitatively very similar results were obtained with a more standard analysis, in which latency was measured based on when firing rates, averaged across trials with the same stimuli, became significantly different to the firing rate in the delay period.

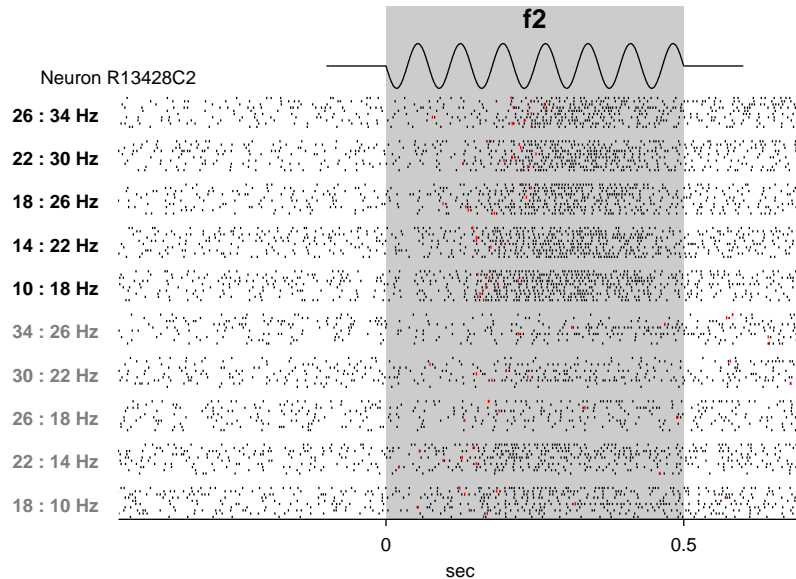


Figure S8. Responses to f_1 of the neuron of Fig. 2 of the main manuscript, with estimated latencies on each trial shown as red tick marks. Mean latency is 186 ms after the start of f_2 ; median latency is 174 ms.

Figure S8 shows, in red tick marks, estimated for each trial of the neuron of Figure 2 in the main text. As can be seen, the method roughly identifies onset latencies that correspond to what is expected visually. However, for some trials, no onset latency is defined. For example, for $(f_1, f_2) = (34, 26)$, only three trials have clear onset latency within the f_2 period, and these latencies are widely different. For other trials [e.g. bottom of the $(14, 22)$ block], firing rate increased to its peak only slowly and smoothly; for these trials also, no particular onset moment could be clearly defined.

Some of the problems with latency measurements are clearly illustrated with the neuron of Figure 3 in the main text. Its responses are shown again in Figure S9 below. For this neuron, no latency can be clearly defined for responses to any of the blocks with $f_2 = f_1 + 8 \text{ Hz}$. Thus, although latency clearly depends on the stimuli for trials with $f_2 = f_1 - 8 \text{ Hz}$, it is impossible, from these data, to determine whether this is a dependence on f_1 alone, f_2 alone, or some combination of the two.

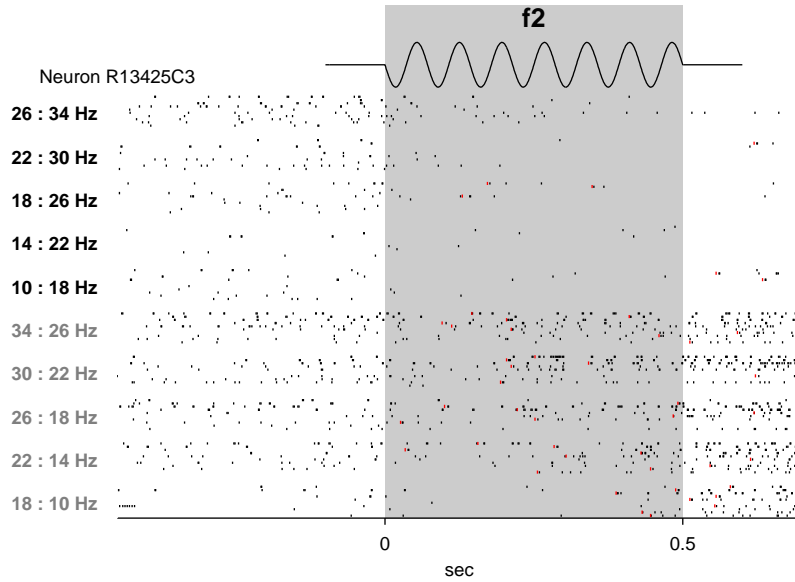


Figure S9. Responses to f_2 of the neuron of Fig. 3 of the main manuscript, with estimated latencies on each trial shown as red tick marks.

For our population latency analysis, we chose only neurons for which latency could be defined for at least 5 trials within each (f_1, f_2) stimulus pair trial type; we further chose only neurons for which these were well-defined latencies for at least three $f_2 > f_1$ trial types and at least three $f_2 < f_1$ trial types. For all neurons that satisfied these criteria, we then fit latency as a linear function of stimulus frequencies:

$$\text{Latency} \sim a_1 * f_1 + a_2 * f_2 + \text{const.}$$

$$\text{latency} = f_1 * a_1 + f_2 * a_2 + \text{const.}$$

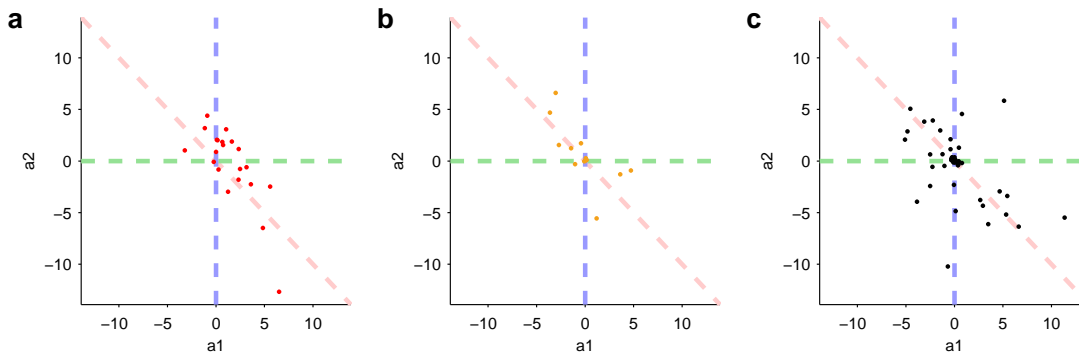


Figure S10. Latency modulations as a function of the applied stimuli. Response onset is fit here for each neuron as a function of stimuli f_1 and f_2 . Each data point represents one neuron. **a**, Neurons classified in Figs. 6 and 7 of main text as ($f_2 - f_1$)-dependent. **b**, Neurons classified in Figs. 6 and 7 as f_2 -dependent. **c**, Neurons classified in Figs. 6 and 7 as intermediate.

The results of this analysis are shown in Figure S10. We do not draw any firm conclusions from it. Very similar results, from which we similarly drew no firm conclusions, were obtained using a more standard latency analysis, in which latency was measured based on when firing rates,

averaged across trials with the same stimuli, became significantly different to the firing rate in the delay period.